AIP | Physics of Plasmas

Flying mirror model for interaction of a super-intense nonadiabatic laser pulse with a thin plasma layer: Dynamics of electrons in a linearly polarized external field

Victor V. Kulagin, Vladimir A. Cherepenin, Min Sup Hur, and Hyyong Suk

Citation: Physics of Plasmas (1994-present) **14**, 113101 (2007); doi: 10.1063/1.2799164

View online: http://dx.doi.org/10.1063/1.2799164

View Table of Contents: http://scitation.aip.org/content/aip/journal/pop/14/11?ver=pdfcov

Published by the AIP Publishing

Flying mirror model for interaction of a super-intense nonadiabatic laser pulse with a thin plasma layer: Dynamics of electrons in a linearly polarized external field

Victor V. Kulagin[a)]
Center for Advanced Accelerators, KERI, Changwon, 641-120, Republic of Korea

Vladimir A. Cherepenin[b)]
Institute of Radioengineering and Electronics of RAS, Mohovaya 11, Moscow 125009, Russia

Min Sup Hur[c)] and Hyyong Suk[d)]
Center for Advanced Accelerators, KERI, Changwon, 641-120, Republic of Korea

(Received 19 June 2007; accepted 24 September 2007; published online 2 November 2007)

Interaction of a high-power laser pulse having a sharp front with a thin plasma layer is considered. General one-dimensional numerical-analytical model is elaborated, in which the plasma layer is represented as a large collection of electron sheets, and a radiation reaction force is derived analytically. Using this model, trajectories of the electrons of the plasma layer are calculated numerically and compared with the electron trajectories obtained in particle-in-cell simulations, and a good agreement is found. Two simplified analytical models are considered, in which only one electron sheet is used, and it moves transversely and longitudinally in the fields of an ion sheet and a laser pulse (longitudinal displacements along the laser beam axis can be considerably larger than the laser wavelength). In the model I, a radiation reaction is included self-consistently, while in the model II a radiation reaction force is omitted. For the two models, analytical solutions for the dynamical parameters of the electron sheet in a linearly polarized laser pulse are derived and compared with the numerical solutions for the central electron sheet (positioned initially in the center) of the real plasma layer, which are calculated from the general numerical-analytical model. This comparison shows that the model II gives better description for the trajectory of the central electron sheet of the real plasma layer, while the model I gives more adequate description for a transverse momentum. Both models show that if the intensity of the laser pulse is high enough, even in the field with a constant amplitude, the electrons undergo not only the transverse oscillations with the period of the laser field, but also large (in comparison with the laser wavelength) longitudinal oscillations with the period, defined by the system parameters and initial conditions of particular oscillation. © *2007 American Institute of Physics*. [DOI: 10.1063/1.2799164]

I. INTRODUCTION

Interaction of super-intense laser pulses with thin foils has been widely investigated during the past decade experimentally,[1–4] analytically,[5–9] and by computer simulations.[10–14] Many interesting physical phenomena have been predicted and observed experimentally in laser-foil interactions. Among them are generation of a high-frequency radiation[13,15] and high harmonics of an incident field,[5,9] production of relativistic electrons[1,2,16] and ions,[14,16,17] generation of relativistic electron mirrors,[15,18–20] shaping of laser pulses[5,21,22] and generation of ultrashort electromagnetic pulses,[23,24] and others. Nevertheless, there is no complete analytical description of all physical processes presented in the interaction of a super-intense laser pulse with a thin plasma layer, so an analytical model for this problem, even phenomenological, is required.

The main instrument for theoretical investigations of the interaction of a super-intense laser pulse with a plasma layer is the particle-in-cell (PIC) simulations. However, this method is inherently numerical and gives only numerical results, so, for developing the analytical model, different approaches are necessary. The fluid model allows the analytical description, but it gives consistent results only for laser pulses with not very high intensity, when the longitudinal displacements of the electrons are small and crossings of electron trajectories do not play an important role.[8,9] When the laser pulse amplitude is large, a numerical-analytical model[19] can be used and it gives adequate results for the quasi-one-dimensional interactions, i.e., for a large enough diameter of the laser beam and small thickness of the plasma layer. This model describes a medium with a large number of electron sheets,[25] and it accounts for the radiation reaction analytically, so the problem can be reduced to the solution of only the equations of motion for the electrons with additional

[a)]On leave from Sternberg Astronomical Institute of Moscow State University, Russia. Present address: APRI, GIST, Gwangju 500-712, Republic of Korea. Electronic mail: victorvkulagin@yandex.ru
[b)]Electronic mail: cher@cplire.ru
[c)]Electronic mail: mshur@keri.re.kr
[d)]Author to whom correspondence should be addressed. Present address: APRI and School of Photon Science and Technology, GIST, Gwangju 500-712, Republic of Korea. Fax: +82-62-970-3419. Electronic mail: hysuk@gist.ac.kr

delayed terms related to the self-action of the plasma-layer radiation field.

In this paper, the general one-dimensional (1D) numerical-analytical model is presented for the interaction of a super-intense laser pulse with a thin plasma layer. Expressions for the radiation reaction force for an ideal infinitely thin electron sheet and for a real plasma layer with finite thickness are elaborated, showing strongly nonlinear character of the longitudinal component of the radiation reaction force. Electron trajectories, calculated in this model, are compared with those in the 1D XOOPIC simulations[26] and a good agreement is ascertained.

As a step toward the development of the complete analytical model for the problem, two simplified analytical models are considered. In both models, there is only one electron sheet, and it moves in the fields of an ion sheet and an ultra-intense laser pulse. Longitudinal displacements of the electrons along the laser beam axis can be considerably greater than the laser wavelength λ in the considered models. This assumption constitutes the main difference of our approach from existing models.[5,8,9,21,22] In model I, called the flying mirror model below (the term "flying mirror" was first used in Ref. 27), the electron sheet radiates an electromagnetic wave when in motion, and this wave modifies the dynamics of the electron sheet so the radiation reaction is included self-consistently here. This model is very important from a physical point of view since it provides the natural mechanism for forgetting the initial conditions (damping) just for only one electron sheet in the system. In the second model II, called the Coulomb model, the radiation of the electron sheet and, hence, the radiation reaction force are omitted. In both models, the analytical solutions are found for the dynamical parameters of the electron sheet in a linearly polarized laser pulse. To elucidate the role of the radiation reaction force in laser interaction with a plasma layer, these analytical solutions are compared for the two models. Also, the analytical solutions for models I and II are compared with the numerical solutions for the central electron sheet (positioned initially in the center) of the real plasma layer, which are calculated from the general numerical-analytical model. Analysis shows that, if crossings of the electron trajectories are unimportant, the trajectory of the central electron sheet can be represented as some combination of the trajectories from models I and II. In general, the Coulomb model gives a better description for the trajectory of the central electron sheet of the real plasma layer, while the flying mirror model gives a better description for the transverse momentum.

Both models show that, even in the external field with a constant amplitude, the electrons undergo large (in comparison with the laser wavelength) longitudinal oscillations with the period, defined by the system parameters and initial conditions of particular oscillation, and also the transverse oscillations with the period of an external field (seen by the electrons). Strong dependence of the trajectory on initial conditions for each longitudinal oscillation gives dynamic stochastization of trajectories just after several longitudinal oscillations even in the considered models, which contain only one electron sheet. This behavior is confirmed for the real thin plasma layer by calculations with the general numerical-analytical model and with the XOOPIC simulations. Dynamics of the electron sheet with omitting the longitudinal part of the radiation reaction force was considered analytically earlier[28] for some cases of electric and magnetic fields.

Below, we will consider the ultra-relativistic laser fields, when the dimensionless amplitude is considerably larger than unity, $a_0=|e|E_0/(mc\omega)\gg 1$, where e and m are the charge and the mass of an electron, c is the speed of light in vacuum, and E_0 and ω are the amplitude and the frequency of an external field.

The paper is organized as follows: In Sec. II, the general numerical-analytical model together with two simplified one-sheet analytical models are considered. In Sec. III, the analytical solutions for the case of large laser pulse amplitudes are found, approximate for model I and exact for model II. In Sec. IV, the evolution of the system in the field of a moderate-intensity electromagnetic wave is considered, and in Sec. V, discussion of the results and conclusions are presented. Details for the derivation of the analytical expressions for the parameters of the electron sheet are presented in the Appendix.

II. MODEL AND MAIN EQUATIONS

A. General model

Let us start with a mathematical model for a motion of an ideal electron sheet, having an infinitely small thickness and a constant surface density of electrons, in an external electromagnetic field. The sheet is supposed to have infinite dimensions in the x and y directions. If the movement of the sheet is without rotations and deformations, then all variables depend only on the coordinate z and time t, and the 1D3V model[25] can be used for the system: the motion of the sheet can be described by three components of velocity $\boldsymbol{\beta}=\mathbf{v}/c$ and one coordinate Z.

Charge and current densities for the electron sheet are $\rho(z,t)=\sigma\delta[z-Z(t)]$ and $\mathbf{j}(z,t)=\sigma\mathbf{v}(t)\delta[z-Z(t)]$, where σ is the surface charge density. Then, formal solutions to Maxwell's equations for the radiation fields of the electron sheet at coordinate z and time t can be obtained with the help of Green function and have the form[19,29]

$$E_z(z,t)=2\pi\sigma\,\mathrm{sign}[z-Z(t')],$$

$$\mathbf{E}_{\perp e}(z,t)=-2\pi\sigma\frac{\boldsymbol{\beta}_\perp(t')}{1-\beta_z(t')\mathrm{sign}[z-Z(t')]},\tag{1}$$

$$\mathbf{H}_e(z,t)=\frac{2\pi\sigma\,\mathrm{sign}[z-Z(t')][\boldsymbol{\beta}_\perp(t')\times\mathbf{e}_z]}{1-\beta_z(t')\mathrm{sign}[z-Z(t')]},$$

where $\mathbf{E}_{\perp e}=E_{xe}\mathbf{e}_x+E_{ye}\mathbf{e}_y$, $\mathbf{v}_\perp=v_x\mathbf{e}_x+v_y\mathbf{e}_y$, and t' is the retarded time

$$c(t-t')=|z-Z(t')|.\tag{2}$$

The expressions (1) are one-dimensional (or, more precisely, 3+1-dimensional) analogs of the classical Lienard-Wiechert solutions[30] and describe the field of an infinite charged (electron) sheet, in which case the field components

E_{ze} and $\mathbf{E}_{\perp e}$ can be interpreted as the near field and the radiation field of the sheet, respectively. From Eqs. (1), one can calculate the self-acting fields for the electron sheet as

$$\mathbf{E}_{\perp es}(Z,t) = -2\pi\sigma\frac{\boldsymbol{\beta}_\perp(t)}{1-\beta_z^2(t)},$$
$$\mathbf{H}_{es}(Z,t) = 2\pi\sigma\beta_z\frac{\boldsymbol{\beta}_\perp(t)\times\mathbf{e}_z}{1-\beta_z^2(t)}. \tag{3}$$

This is the field of a standing wave just at the position of the electron sheet, therefore the amplitude of $\mathbf{E}$ does not equal the amplitude of $\mathbf{H}$. Note that the self-acting field has no longitudinal component. The fields (3) can be represented as the components of an electromagnetic field tensor F^{ik}_{srad} for the self-acting radiation of the sheet. Therefore,

$$F^{ik}_{\text{srad}} = \frac{2\pi\sigma}{1-\beta_z^2}\begin{pmatrix} 0 & \beta_x & \beta_y & 0 \\ -\beta_x & 0 & 0 & -\beta_x\beta_z \\ -\beta_y & 0 & 0 & -\beta_y\beta_z \\ 0 & \beta_x\beta_z & \beta_y\beta_z & 0 \end{pmatrix}. \tag{4}$$

It is easy to check by direct calculations that this is actually a four-tensor, because its components transform from one reference system to another in the same way as the components of a four-tensor must do. The equations of motion for the electrons in the sheet can be obtained in the usual way from the electromagnetic field tensor.[30] For the four-velocity u^i, one has

$$mc\frac{du^i}{ds} = \frac{e}{c}(F^{ik}_{\text{ext}} + F^{ik}_{\text{srad}})u_k = \frac{e}{c}F^{ik}_{\text{ext}}u_k + g^i, \tag{5}$$

where F^{ik}_{ext} is the four-tensor of an external electromagnetic field and $g^i=(e/c)F^{ik}_{\text{srad}}u_k$ is the four-force of the self-action due to the radiation of the sheet. This force is analogous to the Dirac force acting on the moving electron. For an ideal electron sheet, Eq. (5) gives[29,31]

$$\mathbf{F}_{s\perp} = -2\pi\sigma e\boldsymbol{\beta}_\perp,$$
$$F_{sz} = -2\pi\sigma e\beta_\perp^2\beta_z/(1-\beta_z^2). \tag{6}$$

So the radiation reaction force has both transverse $\mathbf{F}_{s\perp}$ and longitudinal F_{sz} components, the latter component being essentially nonlinear. The longitudinal component does not change directly the longitudinal velocity of the sheet[29] [cf. also Eqs. (3)]. This force is only responsible for the change of the longitudinal momentum, according to the change of the mass of the sheet due to the radiation damping of the transverse motion.

For the case of a real plasma layer with finite thickness, the interaction of the electrons with the self-consistent radiation field of the layer gives rise to the effective "viscous" force $\mathbf{F}_s=e\mathbf{E}_s+e\boldsymbol{\beta}\times\mathbf{H}_s$, which acts on each electron in the layer.[29,31] The equations of motion for the electrons have now the following form:

$$\frac{d\mathbf{p}}{dt} = e\mathbf{E} + e\boldsymbol{\beta}\times\mathbf{H} + \mathbf{F}_s, \tag{7}$$

where $\mathbf{p}$ is the relativistic momentum of the electrons, and $\mathbf{E}$ and $\mathbf{H}$ are the external fields (these fields are assumed to be consistent with the model of a medium, which should remain homogeneous in the x and y directions throughout the evolution of the system).

If an initial charge density for the electrons is arbitrarily distributed along the z axis in a region Ω and homogeneous in the x and the y directions, then one can divide Ω into "elementary" electron sheets of width dz_0 by the planes perpendicular to the z axis and describe the state of each sheet by Lagrangian variables. Specifically, let $Z(z_0,t)$ be the longitudinal coordinate of the sheet with the initial coordinate $z_0\in\Omega$ and let $\beta_z(z_0,t)=\partial Z(z_0,t)/c\partial t$ and $\boldsymbol{\beta}_\perp=\boldsymbol{\beta}_\perp(z_0,t)$ be the dimensionless longitudinal and transverse velocities of the sheet. In other words, all electron sheets are numbered by their initial coordinates z_0. For the elementary field of each electron sheet, the expressions in Eqs. (1) are valid; then the total field of the medium is equal to the sum of the fields of the elementary sheets,

$$E_{zs}(z,t) = 2\pi e\int_\Omega n(z_0)\cdot\text{sign}[z-Z(z_0,t)]dz_0,$$
$$\mathbf{E}_{\perp s}(z,t) = -2\pi e\int_\Omega \frac{n(z_0)\cdot\boldsymbol{\beta}_\perp[z_0,t'(z,z_0,t)]}{1-\text{sign}[z-Z(z_0,t)]\cdot\beta_z[z_0,t'(z,z_0,t)]}\times dz_0, \tag{8}$$
$$\mathbf{H}_s(z,t) = 2\pi e\int_\Omega \frac{n(z_0)\cdot\text{sign}[z-Z(z_0,t)]}{1-\text{sign}[z-Z(z_0,t)]\cdot\beta_z[z_0,t'(z,z_0,t)]}\times\boldsymbol{\beta}_\perp[z_0,t'(z,z_0,t)]\times\mathbf{e}_z dz_0,$$

where the retarded time $t'(z,z_0,t)$ is different for different electron sheets and can be determined by Eq. (2).

In many situations, the trajectories of the electron sheets do not cross at least at the initial stage of interaction with a laser pulse (or the number of crossings is insignificant). Then, Eqs. (8) can be greatly simplified. In this case, for the radiation reaction force, acting on the electron sheet with the initial coordinate z_0 from other electron sheets, one has supposing a uniform initial electron density $n(z_0)=n_0$ inside the electron layer of thickness l ($z_0\in[0,l]$)

$$\mathbf{F}_{s\perp}(z_0,t) = -2\pi n_0e^2\{[1-\beta_z(z_0,t)]\mathbf{I}_1 + [1+\beta_z(z_0,t)]\mathbf{I}_2\},$$
$$F_{sz}(z_0,t) = 2\pi n_0e^2\boldsymbol{\beta}_\perp(z_0,t)\cdot(\mathbf{I}_2-\mathbf{I}_1), \tag{9}$$

and

$$\mathbf{I}_1(z_0,t) = \int_{z_0'<z_0}\frac{\boldsymbol{\beta}_\perp[z_0',t'(z_0,z_0',t)]dz_0'}{1-\beta_z[z_0',t'(z_0,z_0',t)]},$$
$$\mathbf{I}_2(z_0,t) = \int_{z_0'>z_0}\frac{\boldsymbol{\beta}_\perp[z_0',t'(z_0,z_0',t)]dz_0'}{1+\beta_z[z_0',t'(z_0,z_0',t)]}. \tag{10}$$

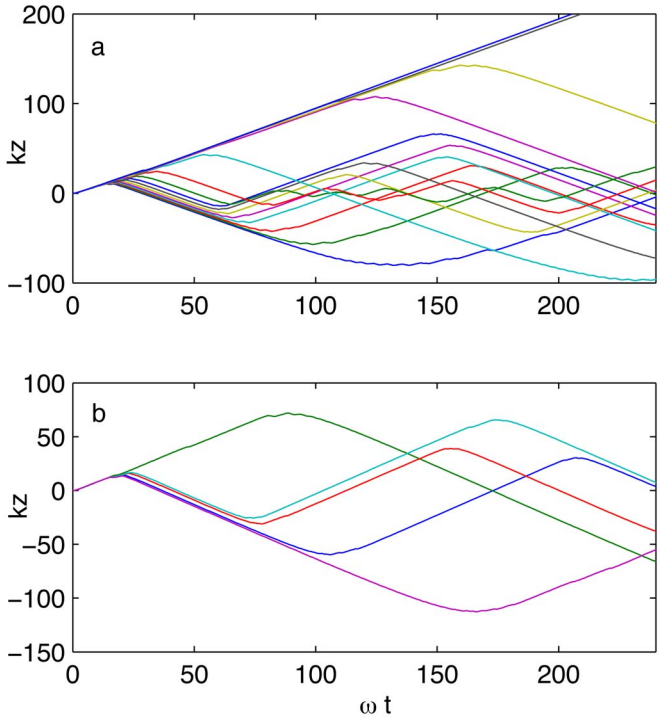

FIG. 1. (Color online) Trajectories of some electrons calculated with the MATLAB code EXACT (a), and through simulations with the 1D XOOPIC code (b). Laser pulse has a step-like envelope with an amplitude $a_0=10$ and parameter $\alpha=2$.

The algorithm for calculation of dynamics for the electron sheets, based on Eqs. (8) together with Eqs. (6), was realized in the MATLAB code EXACT.[19] Some of the trajectories of the electron sheets, which are evenly distributed in the plasma layer initially, are presented in Fig. 1(a). For these calculations, a laser pulse with a step-like envelope and dimensionless amplitude $a_0=10$ was used. The thickness of the plasma layer (10 nm) was considerably smaller than the laser wavelength (1 μ). For such a condition, the dynamics for the electrons of the plasma layer is defined by the product $n_0 l$ rather than by n_0 and l separately. It is convenient to introduce a dimensionless parameter

$$\alpha = \frac{2\pi n_0 l e^2}{mc\omega} = \pi \frac{\omega_p^2}{\omega^2} \frac{l}{\lambda}. \tag{11}$$

The parameter α is the absolute value of the dimensionless Coulomb field of ions acting on the electrons, and $\omega_p = \sqrt{4\pi n_0 e^2/m}$ is the characteristic plasma frequency. In Fig. 1, $\alpha=2$, which corresponds to $n_0 \simeq 7\times 10^{22}$ cm^{-3}.

In Fig. 1(b), the trajectories of test electrons are presented obtained from simulations with the same parameters as in Fig. 1(a), but using the 1D XOOPIC code[26] (modified to monitor trajectories of some test particles). One can conclude that two methods give very similar results for the trajectories of the electrons. Main features for these trajectories are the presence of initial synchronous stage of acceleration of the electrons (e.g., in Fig. 1, it is until $\omega t \simeq 14$) and rapid thermalization of the electrons with high resulting temperature after the termination of the synchronous stage. During synchronous stage, all electron sheets of the plasma layer move with nearly the same velocities without intersections of trajectories, and the radiations of all sheets are added coherently, so the radiation reaction force is maximal on this stage according to Eqs. (9) and (10). Then, electrons on the left side of the bunch are decelerated by the joint Coulomb field of the ion sheets and of the electron sheets from the right side of the bunch. Eventually, these left electron sheets turn back, and the combined radiation reaction force acting on the other electron sheets decreases. The influence of the combined radiation reaction force on the motion of the turned electrons also decreases to a great extent, and only the Coulomb forces take effect for them. This constitutes the cooperative mechanism for decrease of the radiation reaction force in the bunch. In a general case, it is impossible to describe analytically the trajectories of the electrons; only numerical calculations are possible.

B. Model for a single electron sheet in the fields of an ion sheet and a super-intense laser pulse

To get some insight into the peculiarities of the electrons' dynamics, we will consider below the motion of only one electron sheet around the ion sheet (which is supposed motionless) in the field of a super-intense laser pulse. The main emphasis will be made on the role of the radiation-reaction force in this problem, i.e., we will compare two cases—one with the radiation-reaction force and the Coulomb force from the ion sheet (the model I), and the other with the Coulomb force only (the model II). The importance of these models can be substantiated by the following arguments. Let us consider the central electron sheet with initial coordinate $z_0=l/2$ in a thin plasma layer. The central electron sheet can be interesting because, when trajectories do not cross, it corresponds just to the center of distribution (median) of the plasma layer electrons. If $a_0 \gg \alpha$, then for the synchronous stage of evolution (i.e., when the electron sheets have nearly equal velocities, their trajectories do not cross, and the time delay in calculation for total radiation can be ignored), the radiation reaction force acting on the central electron sheet has from Eqs. (9) and (10) components that are exactly equal to the forces, acting on an ideal electron sheet according to Eqs. (6), if one defines the surface electron density σ of this ideal electron sheet through the volume density of electrons, n_0, and the thickness l of the real plasma layer, $\sigma=n_0 l e$. So in this case, model I is applicable. On the other hand, when the radiation reaction force considerably decreases after the termination of the synchronous stage, the Coulomb forces, acting on the central electron sheet from other electron sheets, approximately counterbalance, and the central electron sheet "feels" only the Coulomb forces from the ion sheets (again, this will be true, when it is possible to neglect the crossings of the trajectory of the central electron sheet with the trajectories of the other electron sheets, i.e., during the first longitudinal oscillation), so model II works at this stage. Thus, the trajectory of the central electron sheet in the super-intense laser field can be considered as some combination of the trajectories for the electron sheets from models I and II (at least during the first longitudinal oscillation).

The radiation of the electron sheet in the flying mirror

model is considered in a forthcoming paper.[32] It is necessary to note that the model with a single electron sheet has been intensively developed for a case of a relatively small (but relativistic) amplitude of the laser pulse, $1 \ll a_0 \ll \alpha$ (the so-called sliding mirror model), giving substantial results.[5,21,22,24]

To proceed with the dynamics for the single electron sheet, let an arbitrarily polarized plane electromagnetic wave $\mathbf{E}(\omega t-kz)=E_0\mathbf{e}_{0\perp}(\omega t-kz)$ be incident on this sheet along the z axis ($\mathbf{k}$ is the wave vector of the wave and the function $\mathbf{e}_{0\perp}$ describes the wave envelope). In this case, the dynamics of the sheet can be described by the following equations [cf. Eqs. (6) and (7)]:

$$\frac{dp_x}{dt} = eE_x\left(1-\frac{p_z}{mc\gamma}\right) - \frac{2\pi\sigma e}{mc\gamma}p_x,$$

$$\frac{dp_y}{dt} = eE_y\left(1-\frac{p_z}{mc\gamma}\right) - \frac{2\pi\sigma e}{mc\gamma}p_y,$$

$$\frac{dp_z}{dt} = \frac{e(p_xE_x+p_yE_y)}{mc\gamma} - \frac{2\pi\sigma e}{mc\gamma}\frac{(p_x^2+p_y^2)p_z}{m^2c^2+p_x^2+p_y^2} - 2\pi\sigma e\ \mathrm{sign}\ Z, \tag{12}$$

$$\frac{d\gamma}{dt} = \frac{e(p_xE_x+p_yE_y)}{m^2c^2\gamma} - \frac{2\pi\sigma e}{mc}\frac{p_x^2+p_y^2}{m^2c^2+p_x^2+p_y^2} - \frac{2\pi\sigma e}{m^2c^2\gamma}p_z\ \mathrm{sign}\ Z,$$

$$\frac{dZ}{dt} = \frac{p_z}{m\gamma},$$

where $\gamma=(1-v^2/c^2)^{-1/2}$. Introducing the variable $\kappa=\gamma-p_z/(mc)$, one has for p_z and γ:

$$\gamma = \frac{1+p_x^2+p_y^2+\kappa^2}{2\kappa}, \quad p_z = \frac{1+p_x^2+p_y^2-\kappa^2}{2\kappa}. \tag{13}$$

Here and below, the dimensionless form is used for the momentum $\tilde{p}_{x,y,z}=p_{x,y,z}/(mc)$, and also for the time $\tau=\omega t$ and coordinate $\tilde{Z}=kZ$ instead of the dimensional time t and coordinate Z (for the momenta $\tilde{p}$ and the coordinate $\tilde{Z}$, we use the same symbols p and Z as before). Besides, a variable $\theta=\tau-Z(\tau)$ will be used as an independent variable instead of τ. The transformation is made according to the relation $d/d\tau=[(\gamma-p_z)/\gamma]d/d\theta=(\kappa/\gamma)d/d\theta$ that results in

$$\frac{dp_x}{d\theta} = -a_0e_{0x} - \frac{s\alpha}{\kappa}p_x, \quad \frac{dp_y}{d\theta} = -a_0e_{0y} - \frac{s\alpha}{\kappa}p_y,$$

$$\frac{d\kappa}{d\theta} = \alpha\left(\mathrm{sign}\ Z - s + \frac{s}{1+p_x^2+p_y^2}\right), \quad \frac{dZ}{d\theta} = \frac{p_z}{\kappa}. \tag{14}$$

where the parameter s is equal to 1, if the self-action radiation reaction is present (model I), and zero otherwise (model II), and parameter α is defined by Eq. (11). One can see that α characterizes also the self-radiation reaction force for the electron sheet. The variable Z can be considered just as a switch between two different dynamical solutions to the system (14).

Let us suppose for simplicity that the external wave is linearly polarized and has only x component. For small field amplitudes, one can expect that $p_z \simeq 0$ and

$$\kappa = \sqrt{1+p_x^2}. \tag{15}$$

However, from the system (14), it is apparent that there are no solutions with $p_z \equiv 0$ for the sheet. So in this case, Eq. (15) for κ should be considered as a kind of an averaged relation. The real value for κ executes fast oscillations with a small amplitude near the curve defined by Eq. (15). The period of such oscillations is considerably smaller than the laser period. The evolutions of p_z and Z resemble some kind of sawtooth curves around zero. Physically, this means that the Coulomb forces of the ion remainder are considerably larger than the light pressure force and they can prevent the electrons from the longitudinal displacements.

On the other hand, for large field amplitudes, the light pressure force overcomes the Coulomb force of the ion sheet, and the electrons start to swing longitudinally with large amplitude opposite to the semi-infinite plasma case. For a real plasma layer, such a behavior will be observable, when the amplitude of the longitudinal oscillations will be considerably larger than the thickness of the plasma layer l, i.e., for $a_0 \gg \alpha$ and small l. Also, these oscillations can cause instabilities, e.g., those observed in 1D simulations of Refs. 8 and 9. So the models,[5,8,9,21,22] which suppose that p_z is vanishingly small, can give inconsistent results in the case of large laser pulse amplitudes.

Numerical solutions of Eqs. (14) in the regime of large laser pulse amplitudes, obtained for the step-like laser pulse envelope with $a_0=10$ and $\alpha=2$, are presented in Fig. 2, where trajectories for models I ($s=1$) and II ($s=0$) are shown together with the trajectory of the central electron sheet of the real plasma layer calculated with the code EXACT. Similar electron dynamics can be derived from the PIC simulation in Fig. 1(b) (see also simulations in Refs. 11 and 12).

So when an external electromagnetic wave falls on the system and excites oscillations of the electron sheet, there are two characteristic periods for the motion of the electron sheet—the period of longitudinal oscillations, which is defined either only by the Coulomb field of the ion sheet (model II), or by the radiation reaction force and the Coulomb force (model I), and the period of transverse oscillations, which is equal to the period of the external field (seen by the electron sheet). The dynamics of the electron sheet is determined by the relation between the periods for longitudinal and transverse oscillations and can be very complicated when they are close but not equal.

Equation (14) for the momentum p_x has zero "viscosity" in model II, while, in model I, the viscosity is variable. Actually, for the flying mirror model I, the parameter $\kappa \simeq \kappa_0=1$ for the small times θ, then, the viscosity in the p_x equation is defined by the parameter α and for large α values can be large. When κ grows up, the viscosity coefficient α/κ tends to zero, and the self-radiation reaction force becomes inessential, so the electron sheet effectively "enters" the Coulomb model II. The boundary between two regimes is

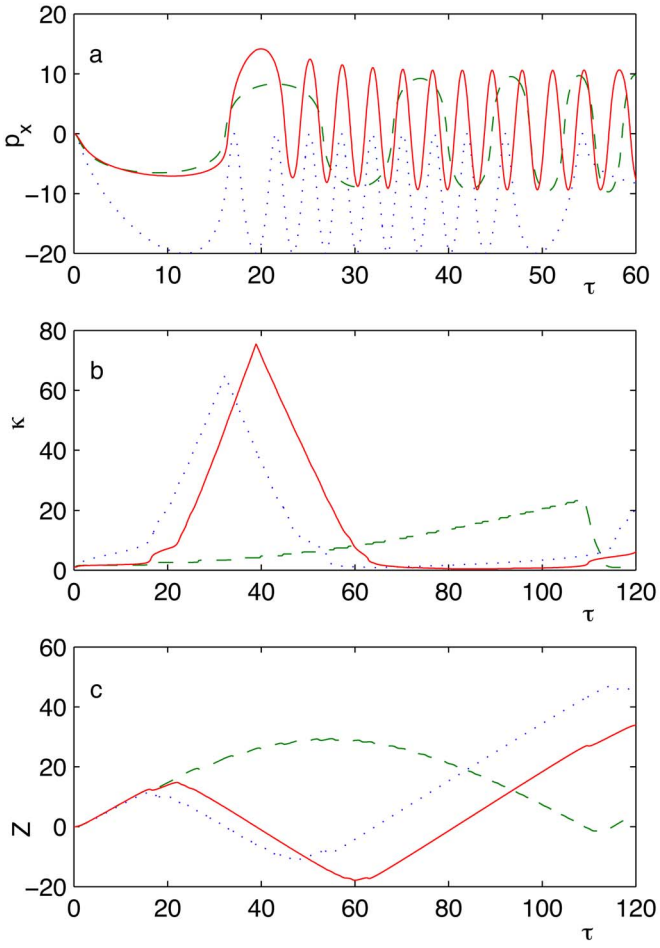

FIG. 2. (Color online) Transverse momentum p_x (a), variable κ (b), and longitudinal coordinate Z (c) for the electron sheet in the field of an intense electromagnetic wave with the step-like amplitude $a_0=10$ for $\alpha=2$ and $\varphi_0=0$: red solid line corresponds to the central electron sheet in the calculations with the EXACT code; green dashed line and blue dotted line are calculated using model I with the radiation reaction ($s=1$) and the model without the radiation reaction (model II, $s=0$) correspondingly. Note different horizontal scales in panel (a) and panels (b) and (c).

$\kappa \sim 5\alpha$ [cf. Eqs. (14)]. Therefore, in model I, the self-radiation reaction force influences on the dynamics of the electron sheet only at the beginning of the longitudinal oscillation; during return part its action is negligible, so the shapes of the trajectories for models I and II coincide here (cf. parts of the trajectories from $\tau \sim 80$ to $\tau \sim 110$ for model I and from $\tau \sim 20$ to $\tau \sim 50$ for model II in Fig. 2). This constitutes an individual mechanism for the decrease of the radiation reaction force in addition to the cooperative mechanism considered in Sec. II B. From the physical point of view, the viscosity provides for "forgetting" the initial conditions of the electron sheet.

III. SOLUTIONS FOR LARGE-FIELD AMPLITUDES

A. Motion in the presence of the radiation reaction force (model I)

1. Approximate solutions for the case $Z>0$

Let us now consider the evolution of the system in more details. When the radiation reaction force is taken into account (model I, $s=1$), the equations of motion (14) become strongly nonlinear, so exact solutions can hardly be written. However, for large external field amplitude $a_0 \gg \alpha$, the momentum p_x can be considered as an oscillating function with slowly changing amplitude and phase (cf. Sec. II B and Fig. 2). So to find approximate solutions, we shall use the slowly varying envelope approximation, i.e., we suppose that the external field has the form

$$a_0(\theta)e_{0x}(\theta) = a_0(\theta)\sin(\theta+\varphi_0), \tag{16}$$

with the amplitude $a_0(\theta)$ of the external field being a slowly varying envelope in comparison with $\sin(\theta+\varphi_0)$, and $\varphi_0=\text{const}$ being an initial phase of the external field. Then, one has for zero initial conditions of p_x (cf. the Appendix)

$$p_x = p_0[\cos(\theta+\varphi_0+\varphi) - \exp(-\alpha\theta/\kappa)\cos(\varphi_0+\varphi)], \tag{17}$$

where

$$p_0 = \frac{a_0\kappa}{\sqrt{\alpha^2+\kappa^2}}, \quad \tan\varphi = \frac{\alpha}{\kappa}, \tag{18}$$

and

$$\kappa = \sqrt{\left(\sqrt{\kappa_0^2+\alpha^2} + \alpha\int_0^\theta \frac{d\theta}{\sqrt{a_0^2+1}}\right)^2 - \alpha^2}. \tag{19}$$

Since the value for κ in Eq. (19) is growing up from the value of κ_0, not only does the amplitude of the oscillations for p_x change during evolution of the system, but the phase of oscillations changes as well.

It is interesting to note that Eqs. (17)–(19) show some delay in solutions clearly visible, e.g., for the laser pulse with a step-like envelope. This delay is similar to a delay of response for a linear oscillator with dissipation. It is the radiation reaction force that provides for such a delay, more exactly, the strongly nonlinear longitudinal component of this force. So this effect is especially important for the large-field amplitudes.

The coordinate Z can be split into two parts—slow Z_s and fast Z_f, and for the step-like amplitude a_0 of the laser field, these parts are defined according to the equations (cf. the Appendix)

$$Z_s = \frac{\theta}{2}\left(\frac{a_0^2}{2\left(\kappa_0^2+\alpha^2+\dfrac{\alpha\theta\sqrt{\kappa_0^2+\alpha^2}}{\sqrt{a_0^2+1}}\right)} - 1\right), \tag{20}$$

$$Z_f = \frac{a_0^2[\sin 2(\theta+\varphi_0+\varphi) - \sin 2(\varphi_0+\varphi)]}{8(\kappa^2+\alpha^2)}. \tag{21}$$

Expression (20) analytically confirms the numerical results of Figs. 1 and 2 showing again that, for large a_0, the longitudinal displacement can be considerably larger than the laser wavelength. Therefore, denoting this fact, the above regime can be called a "flying" regime. Note also the asymmetric character of the longitudinal oscillations for $Z>0$ and $Z<0$ [cf. also Fig. 2(c), green dashed line], which is the result of the interplay between the Coulomb force of the ion remainder and the radiation-reaction force. Due to the nonlinearity of the last, the asymmetry depends on the am-

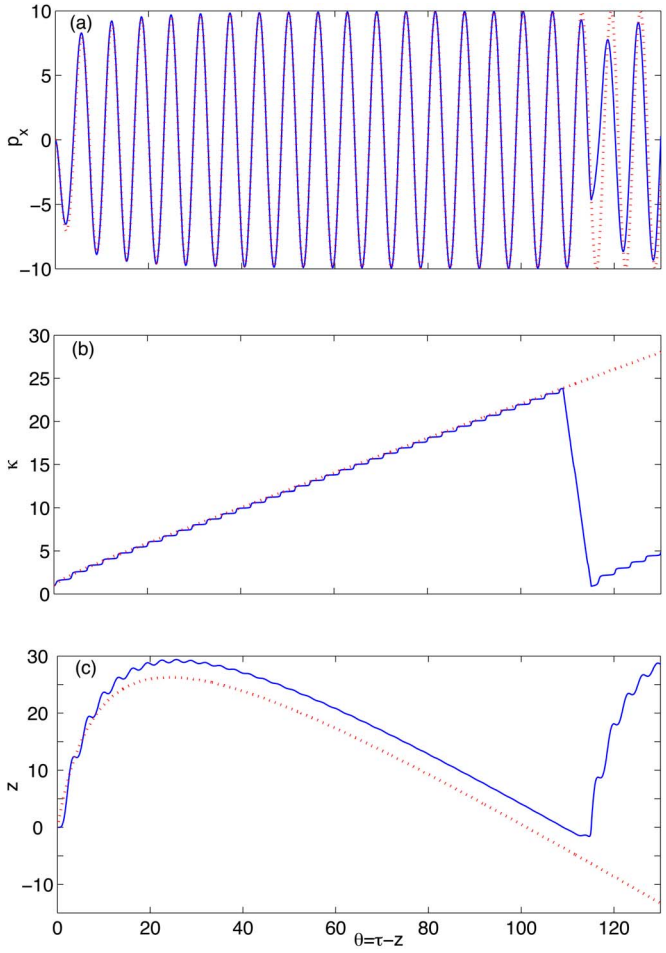

FIG. 3. (Color online) Transverse momentum p_x (a), variable κ (b), and longitudinal coordinate Z (c) for the electron sheet in the field of an intense electromagnetic wave with the step-like amplitude $a_0=10$ for $\alpha=2$ and $\varphi_0=0$ (flying regime, model I). Solid lines (blue) are the numerically calculated results, dotted lines (red) are the approximate solutions according to the expressions (17)–(20).

plitude of the external field. Fast component Z_f decreases with time because of the growth of κ.

In Fig. 3, the approximate solutions (17)–(20) for the first longitudinal oscillation are compared with the numerical solutions to Eqs. (14) in the case of $a_0=10$, $\alpha=2$, $\varphi_0=0$. As can be seen from these figures, the solutions for p_x and κ coincide with good accuracy. The difference in solutions for the coordinate Z is due to neglecting the p_d term in p_x and κ (cf. the Appendix) in calculations of the integral for Z.

Let us estimate at last the period of longitudinal oscillations, θ_l, of the electron sheet in the field of an external electromagnetic wave (the maximal value $Z_{\max}$ of the Z coordinate of the sheet is on the order of $\theta_l/2$ if one disregards the interval where Z goes up). This can be done by equating the coordinate Z_s+Z_f to zero, and, if Z_f can be omitted, gives from expression (20)

$$\theta_l = \frac{\sqrt{a_0^2+1}}{\alpha\sqrt{\kappa_0^2+\alpha^2}}\left(\frac{a_0^2}{2}-\kappa_0^2-\alpha^2\right). \tag{22}$$

The value θ_l depends strongly on the amplitude of the laser field a_0 and on the Coulomb field α, and also, it essentially depends on the parameter κ_0. On the other hand, the value for θ_l from Eq. (22) has no dependence on the initial phase of the laser field φ_0 since the drift term quickly vanishes in the presence of the radiation reaction force.

2. Evolution for the case $Z<0$

In this regime, κ decreases rapidly to the value of about 1. At the same time, the damping α/κ of the transverse momentum grows up [cf. Eq. (14)], and the amplitude of the transverse oscillations decreases. So when the coordinate Z starts to grow after the downfall, the initial values of the system parameters are different from those for the first longitudinal oscillation: $\kappa>0$, $Z=0$, $0\leqslant p_x<a_0$. Besides, the initial phase of the external field φ_0 can be different for the second (and all subsequent) longitudinal oscillation. In this case, the next (and others) longitudinal oscillation can have different duration [cf. Eq. (22) and Figs. 1 and 2]. Also different will be the maximal values for κ and Z; however, the shapes of the dependences on time for the system variables are similar for all longitudinal oscillations. So after several longitudinal oscillations, the variable θ_l and the initial values for p_x, Z, and κ become practically random variables that give dynamic stochastization of the trajectory. This is even more expressed for the variable amplitude $a_0(\theta)$ of an external field, when θ_l (and initial values) change due to the change of $a_0(\theta)$ also. The stochastic motion of a single electron in the field of a super-intense electromagnetic wave was considered earlier.[33,34]

B. Motion in the fields of a laser pulse and an ion sheet (radiation reaction force omitted, model II)

For $Z>0$, one has $[p_x(0)=0]$:

$$p_x(\theta) = -\int_0^\theta a_0(\theta')e_x(\theta')d\theta',$$

$$\kappa(\theta) = \kappa_0 + \alpha\theta, \tag{23}$$

$$Z(\theta) = \int_0^\theta [1+p_x^2(\theta')]d\theta'/[2\kappa^2(\theta')] - \theta/2.$$

For $Z<0$, solutions will be similar, except for κ, which is now a decreasing function of θ: $\kappa(\theta)=\kappa_0-\alpha\theta$, and probably different initial conditions for p_x and κ will be required. Note that the rate of the growth and the decrease for parameter κ are just equal in this case; this ensures symmetry of the electron sheet's trajectory for $Z>0$ and $Z<0$ (cf. Figs. 1 and 2).

To make a comparison with model I, it is convenient to use here for p_x the slowly varying envelope approximation in spite of the availability of the exact solutions (23). Then, one has if a_0 changes slowly

$$p_x = a_0[\cos(\theta+\varphi_0)-\cos\varphi_0]. \tag{24}$$

Important differences here from model I are an absence of the phase modulation for p_x and a constant value for the drift term, which does not decrease with time. Also, the am-

plitude for p_x depends on the amplitude of the external field a_0 only and does not depend on the parameters κ and α.

Based on Eqs. (24), the coordinate Z can be split again into two parts—fast Z_f and slow Z_s. For $\alpha \geqslant 1$, Z_f cannot be neglected, and integral cosine and sine functions can be utilized to calculate Z_f. If $\alpha \ll 1$, Z_f gives only small oscillations, and the total coordinate can be approximated by the slow part Z_s. In this case, one has for the step-like amplitude of the laser pulse

$$Z_s = \frac{\theta}{2}\left(\frac{1 + a_0^2(1/2 + \cos^2\varphi_0)}{\kappa_0(\kappa_0 + \alpha\theta)} - 1\right),$$
$$Z_f = \frac{a_0^2[\sin 2(\theta + \varphi_0) - 8\cos\varphi_0 \sin(\theta + \varphi_0) + 3\sin 2\varphi_0]}{8(\kappa_0 + \alpha\theta)^2}. \tag{25}$$

The period of longitudinal oscillations, θ_l, now has the form

$$\theta_l = \frac{1 - \kappa_0^2 + a_0^2(1/2 + \cos^2\varphi_0)}{\alpha\kappa_0}, \tag{26}$$

so θ_l depends not only on the initial value for κ but on the initial phase φ_0 of the laser field also. The maximal value for θ_l will be achieved for $\varphi_0 = 0$. It is easy to check that even this maximal value for θ_l is smaller than the value for θ_l from Eqs. (22) for model I (with the radiation reaction), so the radiation reaction force provides additional longitudinal acceleration for the electron sheet. The physical mechanism for such a phenomenon was considered in Refs. 19 and 29.

IV. EVOLUTION OF THE SYSTEM IN THE FIELD OF A MODERATE-INTENSITY ELECTROMAGNETIC WAVE

To define the meaning of the definition "moderate," let us analyze expression (22) for the period of the longitudinal oscillations for the electron sheet. It can be seen that when

$$a_0 \leqslant \sqrt{2(\kappa_0^2 + \alpha^2)}, \tag{27}$$

θ_l and $Z_{\max}$ become considerably smaller than the period of the external field and the laser wavelength correspondingly. Then, the electron sheet can be considered as practically motionless in the z direction for $a_0 < \alpha\sqrt{2}$ (supposed $\alpha \gg \kappa_0$), and only the equation for p_x from the system (14) should be solved, with the parameter κ approximately determined according to Eq. (15) (cf. Sec. II B). So the regime of small or large amplitudes of the external wave can be defined by the fulfillment of the inequality (27) or the opposite one.

For the Coulomb model II, the momentum p_x does not depend on κ so, for small laser pulse amplitudes, the solution for p_x is given just by Eqs. (23), and the solution for κ is given by Eq. (15). So below, we shall consider the solutions for the flying mirror model I, which accounts for the radiation reaction.

If p_x is small ($a_0 \ll \alpha$), then $\kappa = \sqrt{1 + p_x^2} \simeq 1$, and the momentum p_x undergoes the evolution with the full viscosity equal to α. So this regime can be called a "viscous," or "damped," regime, contrary to the flying regime considered in Sec. III A, in which the viscosity in the equation for p_x tends to zero when κ grows.

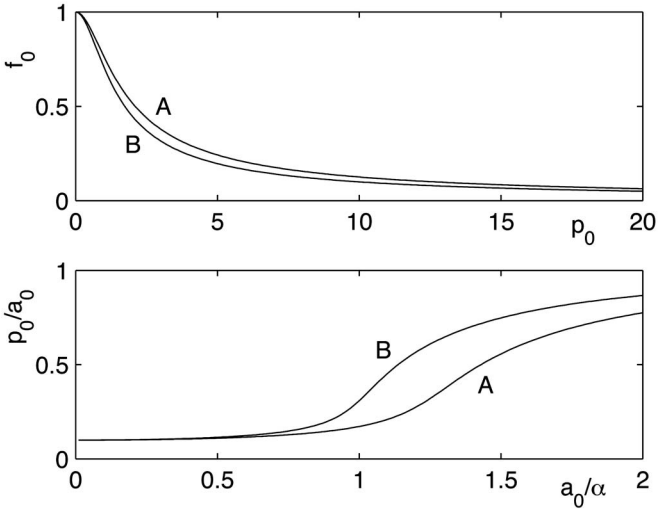

FIG. 4. Comparison of two approximations for the function $f_0 = f(p_0)$ (a) [curve A, numerical calculation of the integral (29); curve B, approximation according to Eq. (30)], and the amplitude p_0 (b) [curve A, numerical solution from Eqs. (28); curve B, approximate solution from Eq. (31)].

Let the solution for p_x be written again as in Eq. (A1). With the help of the averaging method used above, one can obtain for $\alpha \geqslant a_0 \geqslant 1$ the following equations (zero initial condition for p_x is supposed):

$$p_0^2[1 + \alpha^2 f(p_0)^2] = a_0^2, \quad \tan\varphi = \alpha f(p_0),$$
$$p_d = -p_0 \exp(-\alpha\theta)\cos(\varphi_0 + \varphi), \tag{28}$$

where the function $f(p_0)$ is defined according to the equation

$$f(p_0) = \frac{1}{\pi}\int_0^{2\pi} \frac{\cos^2\theta d\theta}{\sqrt{1 + p_0^2\cos^2\theta}}, \tag{29}$$

and p_0 has to be considered as constant in this integral. Function $f(p_0)$ can be written in the analytic form as a sum of elliptic integrals depending on an imaginary argument. Also, for $f(p_0)$, the following inequalities are valid:

$$1 \geqslant f(p_0) \geqslant (1 + p_0^2)^{-1/2}. \tag{30}$$

The values $f(p_0) \simeq 1$ are achieved for the small momenta $p_0 \ll 1$ that corresponds to the inequality $a_0 \ll \alpha$. For relatively large values of p_0, corresponding to the regime $a_0 \sim \alpha$, the reasonable approximation for the function $f(p_0)$ can be $f(p_0) \simeq (1 + p_0^2)^{-1/2}$. This dependence is presented in Fig. 4(a) (curve B), together with the numerical calculations for the function $f(p_0)$ according to Eq. (29) (curve A), and a relatively good agreement can be ascertained. Using the approximation $f(p_0) \approx (1 + p_0^2)^{-1/2}$, one can obtain the approximate analytic expression for p_0,

$$p_0^2 = [\sqrt{(a_0^2 - \alpha^2 - 1)^2 + 4a_0^2} + a_0^2 - \alpha^2 - 1]/2. \tag{31}$$

Comparison of two approximations for the amplitude p_0, obtained from the numerical solution of the first equation of Eqs. (28) and from Eq. (31), is presented in Fig. 4(b) ($\alpha = 10$). Two curves are close enough for the case $a_0 \leqslant \alpha$, however, for $\alpha \leqslant a_0 \leqslant \alpha\sqrt{2}$, the approximation (31) gives only qualitative results for a linearly polarized external field.

The dependences in Fig. 4(b) demonstrate highly nonlinear behavior of the momentum amplitude p_0 with respect to the laser field amplitude a_0. This feature can be effectively used for shaping the laser pulses[5,21,22] that will be considered in detail in a forthcoming paper.[32]

V. DISCUSSION OF RESULTS AND CONCLUSIONS

From Fig. 2, one can conclude that the parameters of motion (p_x, κ, and Z) for the central electron sheet of the plasma layer coincide well with the predictions of model I (with the radiation reaction) at the initial stage of interaction (until $\omega t \simeq 20$ for parameters used in simulation, $a_0=10$, $\alpha=2$). After that, the role of the radiation reaction force decreases due to cooperative and individual mechanisms, and the evolution of the trajectory of the central electron sheet resembles the evolution of the electron sheet's trajectory in the Coulomb model II. Thus, the trajectory has almost triangular form as opposed to the model I with a parabolic shape of the trajectory [Fig. 2(c)], and the durations of the first longitudinal oscillation are close (about 39 for the central electron sheet in the numerical-analytical model and 32 for the model II as opposed to 110 in the model I).

However, the Coulomb model II has some shortcoming for full description of the process. Namely, in this model, the drift term in the transverse momentum p_x exists for infinite time, so the initial conditions cannot be forgotten. Besides, the maximal absolute value for p_x is overestimated in this model: for simulations of Fig. 2, the overestimation is by two times. But for the case of $a_0 \leqslant \alpha$, the overestimation can be more considerable, e.g., for $a_0=5$, $\alpha=10$, the XOOPIC and the EXACT simulations give $|p_x|_{\max} \simeq 0.55$, the model with the radiation reaction force (model I) gives $|p_x|_{\max} \simeq 0.56$ (cf. Fig. 4), while model II gives $|p_x|_{\max}=10$. Note that in the flying mirror model I, there is a natural physical mechanism for the forgetting the initial conditions: this is the radiation of the electron sheet, which is self-consistently included in the model, that is why this model correctly describes the evolutions of the amplitude and the drift term of p_x [cf. Fig. 2(a)]. So future efforts in the developing the general analytical model may be successful through an inclusion into the flying mirror model of a mechanism for a gradual suppression of the radiation reaction force on later stages of evolution (equivalent to cooperative mechanism, cf. Sec. II A) in addition to the inherent decrease due to the growth of κ (individual mechanism, cf. Sec. II B).

The step-like laser pulse envelope was considered in the analytical models above. For the external wave with a time dependent amplitude (laser pulse with finite duration), the longitudinal displacement of the electron sheet is negligible at once. Then, with growing the field amplitude, the longitudinal displacement increases, and the sheet undergoes several large longitudinal oscillations with parameters depending on the pulse duration and the maximal amplitude of the field. After that, the amplitude of the longitudinal displacements tends to zero at the back end of the laser pulse. The initial conditions for the large longitudinal oscillations become practically random in this case, because, before large longitudinal oscillations, the sheet undergoes a great number of small oscillations along z (with the amplitude less than the laser wavelength). For the laser pulses with moderate maximal field amplitudes, the situation is still more complicated, and for $(a_0)_{\max} \sim \alpha\sqrt{2}$ the motion of the electrons can resemble the stochastic behavior.

In conclusion, the analytical model with only one electron sheet moving in the fields of an ion sheet and a laser pulse was considered above as the step toward the development of the full analytical model for the problem. Inside this one-sheet model, two cases were considered and compared with the characteristics of the central electron sheet in the real plasma layer—the flying mirror model I includes the radiation reaction force, while this force is omitted in the Coulomb model II. For both cases, the analytical solutions for the dynamical parameters of the electrons were found (approximate for the model I and exact for the model II). In general, the Coulomb model II gives better description for the trajectory Z and the parameter κ of the central electron sheet of the real plasma layer, however the transverse momentum p_x is better described by the flying mirror model I.

It is possible to distinguish two regimes in the dynamics of the electron sheet in a super-intense laser field for large parameter α: flying regime ($a_0 \geqslant \alpha\sqrt{2}$), which is characterized by the large longitudinal oscillations of the electrons (with amplitude considerably larger than λ), and viscous, or damping, regime ($a_0 \leqslant \alpha\sqrt{2}$) when the longitudinal displacements are smaller than λ. In both regimes, the electrons undergo also the transverse oscillations with the period of the external field. The period of longitudinal oscillations is defined by the system parameters a_0 and α, and also it depends essentially on the initial conditions of each oscillation (which after some time of evolution become random variables), which results in variation of this period from one longitudinal oscillation to another. This feature contrasts with the case of a semi-infinite plasma, where only a small part of the electrons has a large amplitude of longitudinal motion.

ACKNOWLEDGMENTS

We thank S. V. Bulanov for stimulating discussions and valuable comments. This work was supported by the Creative Research Initiative Program of the Korean Ministry of Science and Technology.

APPENDIX: SOLUTIONS IN MODEL I FOR LARGE-FIELD AMPLITUDES AND $Z>0$

We suppose that the solution for p_x can be written in the following form:

$$p_x = p_d + p_0 \cos(\theta + \varphi_0 + \varphi), \tag{A1}$$

where p_d, p_0, and φ are the slowly varying functions of variable θ. Then, one can obtain using the slowly varying envelope approximation

$$\frac{dp_d}{d\theta} = -\frac{\alpha}{\kappa} p_d, \quad p_0 = \frac{a_0\kappa}{\sqrt{\alpha^2+\kappa^2}}, \quad \tan\varphi = \alpha/\kappa,$$
$$\frac{d\kappa}{d\theta} = \frac{\alpha}{\sqrt{1+p_0^2}} = \alpha\sqrt{\frac{\alpha^2+\kappa^2}{\alpha^2+\kappa^2(a_0^2+1)}}, \tag{A2}$$

where the part due to p_d was omitted in κ. Expanding the square root in the equation for κ into Taylor series with keeping only the linear term in $\alpha^2/\kappa^2(a_0^2+1)$ and omitting the logarithmic terms in the resulting integral, one can get expression (19) for κ.

To find the drift term p_d, let us at first consider κ as being constant. Then, for $p_x(0)=0$, one has

$$p_d = -p_0\cos(\varphi_0+\varphi)\exp(-\alpha\theta/\kappa). \tag{A3}$$

From this solution, one can conclude that the function p_d changes much faster with θ than the function κ. So one can use the solution (A3) not only for the constant value of κ, but for the changing κ as well. Then, the full solution for the momentum p_x acquires the form of Eq. (17).

For the long-term evolution of the longitudinal coordinate of the sheet (evolution for large θ values), one can omit in p_x the exponential terms arising from p_d. Then, the longitudinal coordinate Z can be split into two parts—slow Z_s and fast Z_f, and the following equations are valid:

$$\frac{dZ_s}{d\theta} = \frac{2+p_0^2}{4\kappa^2} - \frac{1}{2},$$
$$\frac{dZ_f}{d\theta} = \frac{p_0^2\cos 2(\theta+\varphi_0+\varphi)}{4\kappa^2}, \tag{A4}$$

and during integration of the second equation of (A4), the variables p_0, κ, and φ have to be considered as constants. The equation for Z_s cannot be integrated without a selection of an explicit expression for $a(\theta)$. For the step-like amplitude $a(\theta)$, one can obtain Z_s in the form of Eq. (20).

[1] P. Audebert, R. Shepherd, K. B. Fournier, O. Peyrusse, D. Price, R. W. Lee, P. Springer, J.-C. Gauthier, and L. Klein, Phys. Rev. E **66**, 066412 (2002).
[2] Y. T. Li, J. Zhang, L. M. Chen *et al.*, Phys. Rev. E **64**, 046407 (2001).
[3] D. Giulietti, L. A. Gizzi, A. Giulietti, A. Macchi, D. Teychenne, P. Chessa, A. Rousse, G. Cheriaux, J. P. Chambaret, and G. Darpentigny, Phys. Rev. Lett. **79**, 3194 (1997).
[4] J. Fuchs, J. C. Adam, F. Amiranoff *et al.*, Phys. Plasmas **6**, 2569 (1999).
[5] V. A. Vshivkov, N. M. Naumova, F. Pegoraro, and S. V. Bulanov, Phys. Plasmas **5**, 2727 (1998).
[6] V. V. Goloviznin and T. J. Schep, Phys. Plasmas **7**, 1564 (2000).
[7] Sh. Amiranashvili, M. Y. Yu, and L. Stenflo, Phys. Plasmas **10**, 1239 (2003).
[8] B. Shen and Z. Xu, Phys. Rev. E **64**, 056406 (2001).
[9] B. Shen and J. Meyer-ter-Vehn, Phys. Plasmas **8**, 1003 (2001).
[10] K. Nagashima, Y. Kishimoto, and H. Takuma, Phys. Rev. E **58**, 4937 (1998).
[11] E. Lefebvre and G. Bonnaud, Phys. Rev. E **55**, 1011 (1997).
[12] R. A. Cairns, B. Rau, and M. Airila, Phys. Plasmas **7**, 3736 (2000).
[13] A. Zhidkov, J. Koga, A. Sasaki, and M. Uesaka, Phys. Rev. Lett. **88**, 185002 (2002).
[14] Y. Sentoku, T. E. Cowan, A. Kemp, and H. Ruhl, Phys. Plasmas **10**, 2009 (2003).
[15] V. A. Cherepenin and V. V. Kulagin, Phys. Lett. A **321**, 103 (2004).
[16] W. Yu, V. Bychenkov, Y. Sentoku, M. Y. Yu, Z. M. Sheng, and K. Mima, Phys. Rev. Lett. **85**, 570 (2000).
[17] A. Zhidkov and A. Sasaki, Phys. Plasmas **7**, 1341 (2000).
[18] B. Rau, T. Tajima, and H. Hojo, Phys. Rev. Lett. **78**, 3310 (1997).
[19] V. A. Cherepenin, A. S. Il'in, and V. V. Kulagin, Fiz. Plazmy **27**, 1111 (2001) [Plasma Phys. Rep. **27**, 1048 (2001)].
[20] K. Nagashima, Y. Kishimoto, and H. Takuma, Phys. Rev. E **59**, 1263 (1999).
[21] S. V. Bulanov, T. J. Esirkepov, N. M. Naumova, F. Pegoraro, I. V. Pogorelsky, and A. M. Pukhov, IEEE Trans. Plasma Sci. **24**, 393 (1996).
[22] S. V. Bulanov, A. Macchi, and F. Pegoraro, Phys. Lett. A **245**, 439 (1998).
[23] D. Bauer, R. R. E. Salomaa, and P. Mulser, Phys. Rev. E **58**, 2436 (1998).
[24] A. S. Pirozhkov, S. V. Bulanov, T. Zh. Esirkepov, M. Mori, A. Sagisaka, and H. Daido, Phys. Lett. A **349**, 256 (2006).
[25] C. K. Birdsall and A. B. Langdon, *Plasma Physics Via Computer Simulation* (MacGraw-Hill Book Company, New York, 1985), p. 8.
[26] H. Usui, J. P. Verboncoeur, and C. K. Birdsall, IEICE Trans. Electron. **E83C**, 989 (2000).
[27] S. V. Bulanov, T. Esirkepov, and T. Tajima, Phys. Rev. Lett. **91**, 085001 (2003).
[28] S. V. Bulanov, Izv. Vyssh. Uchebn. Zaved., Radiofiz. **18**, 1511 (1975).
[29] A. S. Il'in, V. V. Kulagin, and V. A. Cherepenin, Radiotekh. Elektron. (Moscow) **44**, 389 (1999) [J. Commun. Technol. Electron. **44**, 385 (1999)].
[30] L. D. Landau and E. M. Lifshitz, *The Classical Theory of Fields* (Nauka, Moscow, 1988), p. 212.
[31] V. L. Bratman and S. V. Samsonov, Phys. Lett. A **206**, 377 (1995).
[32] V. V. Kulagin, V. A. Cherepenin, M. S. Hur, and H. Suk, Phys. Plasmas **14**, 113102 (2007).
[33] J. M. Rax, Phys. Fluids B **4**, 3962 (1992).
[34] D. Bauer, P. Mulser, and W.-H. Steeb, Phys. Rev. Lett. **75**, 4622 (1995).